ISSN: 2414-1895 DOI: 10.6919/ICJE.202502_11(2).0019

Novel Conjugated Bipolar Molecules for Organic Redox Flow Batteries

Yunjie Cao[a], Chengxin Peng[*]

University of Shanghai for Science and Technology, Shanghai 200093, China

[a]222203118@st.usst.edu.cn, [*]cxpeng@usst.edu.cn

Abstract

Developing a symmetrical redox flow battery that utilizes the same electroactive material for both the anode and cathode could significantly simplify the manufacturing process and reduce costs. However, the reported bipolar molecules exhibit low voltages(typically below 2V), and the challenge lies in finding suitable bipolar active molecules, which are barriers to the realization of bipolar redox flow batteries. Herein, we have developed a novel molecular strategy that involves the fusion of appropriate p-type and n-type redox materials to create bipolar molecules. Through which, electronic perturbations between the anodic and cathodic active sites lead to an effective voltage shift, enabling higher voltages in symmetrical batteries. We demonstrate the newly designed OBO molecules(where O and B are redox centers), which successfully exhibits bipolar redox activity and provides a high discharge voltage of approximately 3.05V in symmetrical batteries, one of the highest values reported to date. This simple conjugation approach offers a new perspective for the design of high-voltage, high-energy-density bipolar redox materials.

Keywords

Bipolar Redox Flow Batteries; Fusion; High Discharge Voltage.

1. Introduction

In the realm of electrochemical energy storage, redox organic molecules (ROMs) are favored over their inorganic counterparts due to their structural diversity and tunability, rendering them as prime candidates for the development of sustainable redox flow batteries (RFBs) for large-scale applications [1]. The aqueous electrolytes employed in conventional RFBs are limited by their narrow electrochemical windows, which impede the high energy density of RFBs. In contrast, non-aqueous electrolytes, with their expanded electrochemical windows, provides the possibility for ROMs to achieve functional diversity. Therefore, non-aqueous RFBs exhibit unique advantages in energy storage systems. Recently, a number of non-aqueous RFBs systems have been reported. However, most of them suffer from serious electrolyte crossover. This is due to the poor ion selectivity of the porous membranes used [2]. Consequently, it triggers electrolyte crossover and leads to irreversible capacity loss, battery failure, and even safety hazards.

To solve this issue, an effective strategy is to use a symmetric battery rather than the traditional asymmetric battery structure. In the symmetric battery structure, the posolyte and negolyte use the same supporting electrolyte and bipolar ROMs, which can effectively alleviate the electrolyte cross-contamination problem due to chemical gradients, and thus reduce the capacity degradation of the battery. Various strategies have been intensively investigated to realize symmetric ORFBs, such as the formation of bipolar deep eutectics mixtures [3], and the construction of bipolar molecules by covalently bonding positive and negative active materials [4]. However, the voltage of symmetric

ISSN: 2414-1895 DOI: 10.6919/ICJE.202502_11(2).0019

ORFBs constructed in these two types of ways usually does not exceed 2V, and the energy density is low. Another approach is to conjugate fusion of p-type and n-type materials in a single structure to achieve a wider voltage gap through intrinsic electronic perturbations [5]. In principle, this will facilitate the realization of higher output voltages, thereby increasing the energy and power density of the ORFBs.

In this study, we propose an effective design strategy that involves the conjugation fusion of an electron-withdrawing group B with an electron-donating group O within the same molecule OBO. The successful synthesis is confirmed by nuclear magnetic resonance (NMR) ^{1}H and ^{13}C spectra. This bipolar molecule has a voltage gap of up to 3.1V and exhibits good cycling stability in electrochemical CV testing. The assembled flow battery exhibited a high discharge platform of 3.05V and maintained a Coulombic efficiency (CE) of 80% over 100 cycles. Our work brings innovative perspectives to bipolar ROM design, which can improve the voltage stability and overall performance of symmetric ORFBs.

2. Experimental Section

2.1 Synthetic Procedures

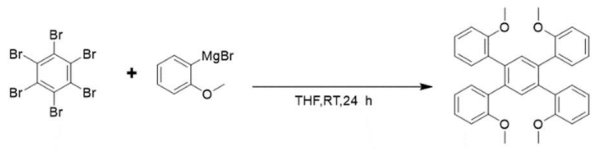

Figure 1. Synthesis procedure of OBO-OMe

To a Schlenk flask containing hexabromobenzene (5.52 g, 10.0 mmol), a solution of (2-methoxyphenyl)magnesium bromide (1.0 M, 80 mL, 80 mmol) in THF was introduced under an argon atmosphere. The reaction mixture was stirred at ambient temperature for 24 hours, followed by quenching with a solution of ice and dilute hydrochloric acid. Subsequently, the mixture was extracted with chloroform in three separate operations. The combined organic phases were washed successively with brine and water, then dried over magnesium sulfate ($MgSO_4$). After the solvent was evaporated under reduced pressure, the resulting residue was subjected to column chromatography on silica gel using a hexane/dichloromethane (1:1) eluent to isolate the product. Further purification involved washing with hexane and a minimal amount of toluene (3 mL), yielding 1.61 g (40%) of compound OBO-OMe as a white solid. ^{1}H NMR (500 MHz, $CDCl_3$) δ 7.48 (s, 2H), 7.19 – 7.11 (m, 8H), 6.82 (t, J = 7.4 Hz, 4H), 6.73 (d, J = 8.3 Hz, 4H), 3.46 (s, 12H); ^{13}C NMR (126 MHz, $CDCl_3$) δ 156.45, 131.82, 127.93, 120.00, 110.40, 55.05.

Figure 2. Synthesis procedure of OBO

To a solution of compound OBO-OMe (201 mg, 0.400 mmol) in anhydrous dichlorobenzene (20 mL), BBr_3 (1.0 M in heptane, 1.2 mL, 1.2 mmol) was added under an argon atmosphere. The reaction mixture was then heated to 150 °C and maintained at this temperature with stirring for 12 hours. After quenching with methanol, the reaction mixture was concentrated under reduced pressure. The residue was subsequently purified by column chromatography over silica gel using a hexane/dichloromethane (1:1) eluent. The product was further recrystallized from from CH_2Cl_2/MeOH to yield 170 mg (92%) of compound OBO as a yellow solid. ^{1}H NMR (500 MHz, $CDCl_3$) δ 8.27 (d, J = 8.1 Hz, 4H), 7.48

ISSN: 2414-1895 DOI: 10.6919/ICJE.202502_11(2).0019

(d, J = 8.3 Hz, 4H), 7.40 (t, J = 7.8 Hz, 4H), 7.04 (t, J = 7.6 Hz, 4H); ^{13}C NMR (126 MHz, $CDCl_3$) δ 151.52, 132.70, 130.08, 128.84, 122.96, 122.19, 120.35.

2.2 NMR Spectra

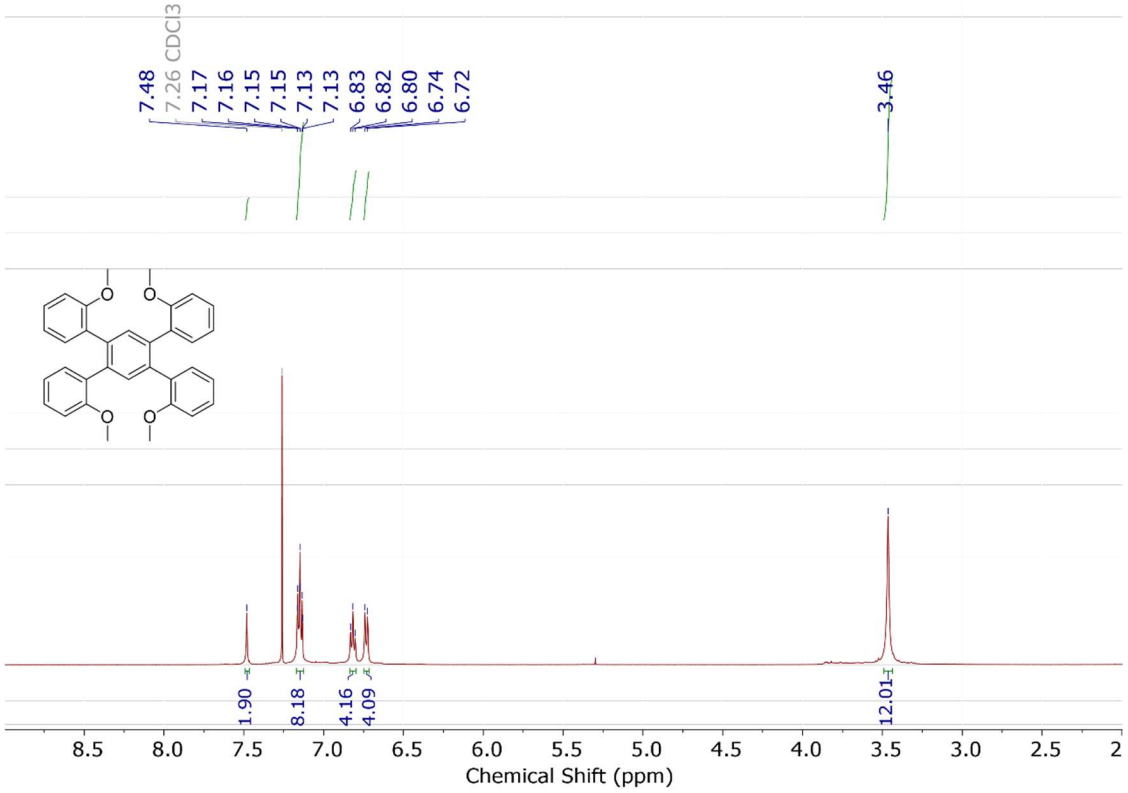

Figure 3. ^{1}H NMR spectrum of OBO-Ome

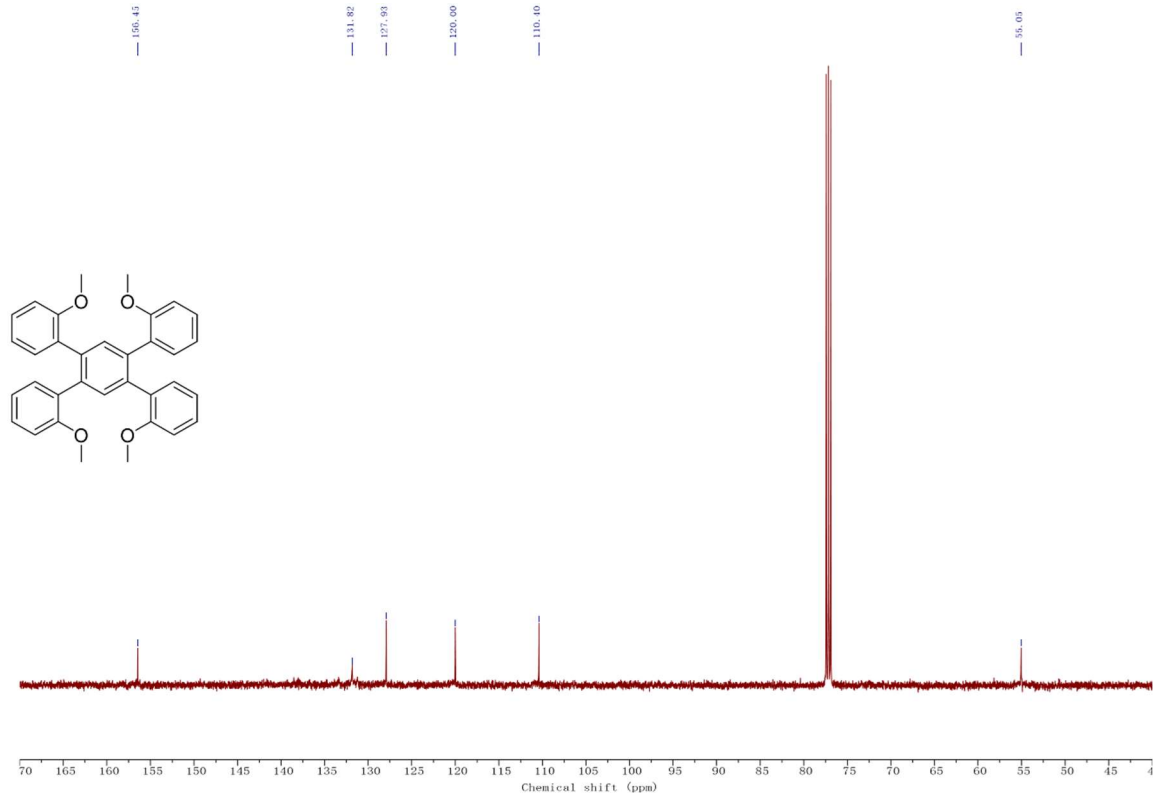

Figure 4. ^{13}C NMR spectrum of OBO-OMe

ISSN: 2414-1895 DOI: 10.6919/ICJE.202502_11(2).0019

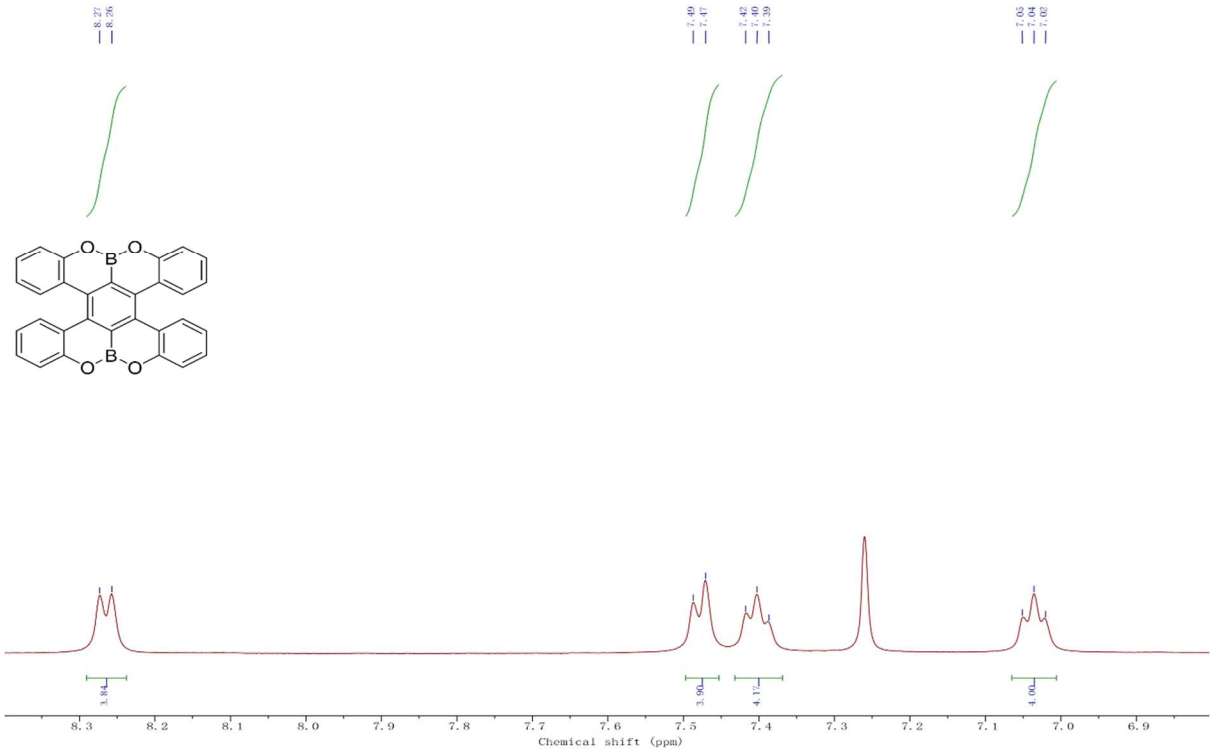

Figure 5. ^{1}H NMR spectrum of OBO

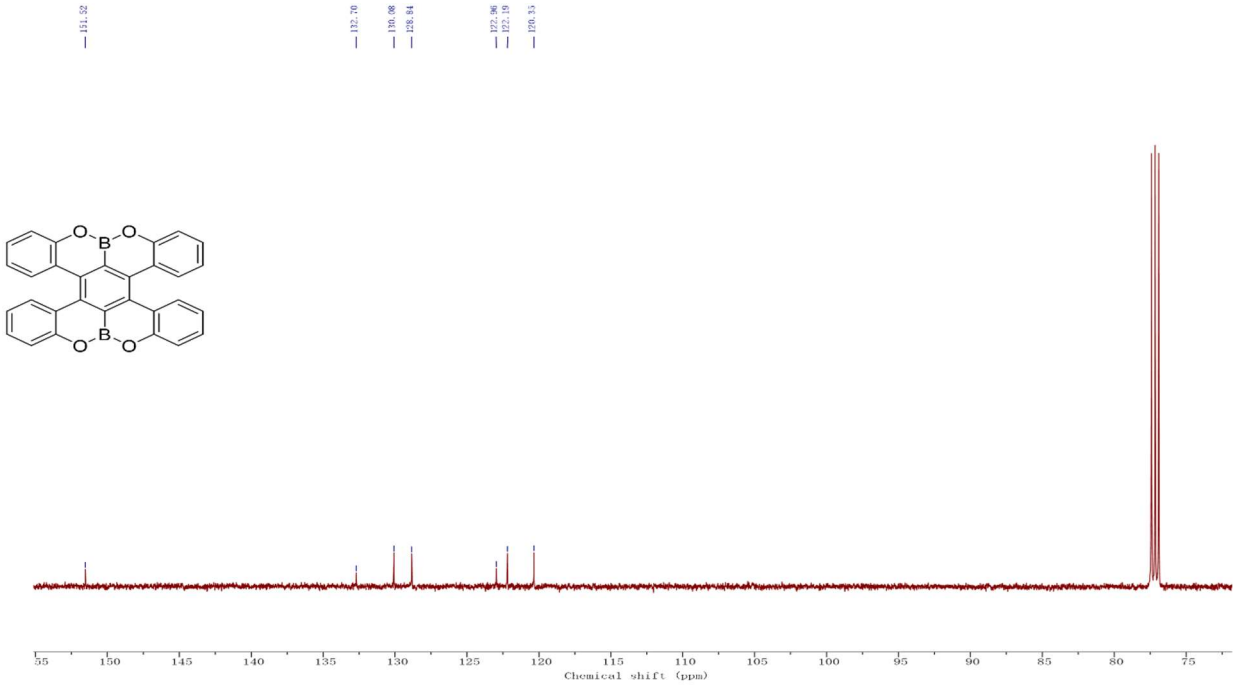

Figure 6. ^{13}C NMR spectrum of OBO

3. Results and Discussion

In essence, n-type O atom and p-type B atom are employed as the anode-active and cathode-active centers, respectively, to engineer bipolar redox organic materials (ROMs). Upon the fusion of the two redox-active moieties into a unified conjugated system, the electron density surrounding the O atom is diminished due to the electron-withdrawing influence exerted by the para B atom. Simultaneously, the electron density in the vicinity of the B atom is augmented by the electron-donating effect of the para O atom, which harbors a lone pair of electrons in a p-orbital oriented perpendicular to the plane

ISSN: 2414-1895 DOI: 10.6919/ICJE.202502_11(2).0019

of conjugation. During an oxidation event, a higher potential is requisite to extract an electron from the p orbital of oxygen (O), as the negative charge compensation is impeded by the electron-withdrawing boron (B) atom, leading to an elevation in the oxidation voltage. Similarly, during a reduction event, a lower potential is sufficient for the boron (B) atom to accept an electron, given that negative charge compensation is facilitated by the electron-donating oxygen (O) atom, resulting in a reduction in the reduction voltage. Therefore, when such kind of BRM is used as both cathode and anode materials in a symmetric RFB, the potential difference between the two half-reactions is enlarged, thus increasing the output voltage of the RFB.

Following this principle, we used a O (electron donor) and a B (electron acceptor) as the redox-active centers and synthesized a bipolar molecule OBO. The main synthesis process along with NMR ^{1}H and ^{13}C was shown in the experimental section (Figure 1-6). Furthermore, we tested the solubility of OBO molecules in acetonitrile (ACN) solutions using UV-vis titrations. As shown in Figure 7a, a standard curve for the molecule OBO was constructed using concentrations of 4, 8, 12, 16, and 20 mg / L. Subsequently, 0.1 mL aliquots of the saturated solutions in acetonitrile were diluted to a final volume of 10 mL. Based on this, linear regression analysis of the absorbance data at various concentrations was performed (Figure 7b), yielding a calculated saturation concentration of OBO in acetonitrile solution to be approximately 3.85 mM. The relatively low solubility is primarily attributed to the larger molecular framework of OBO formed by conjugated fusion.

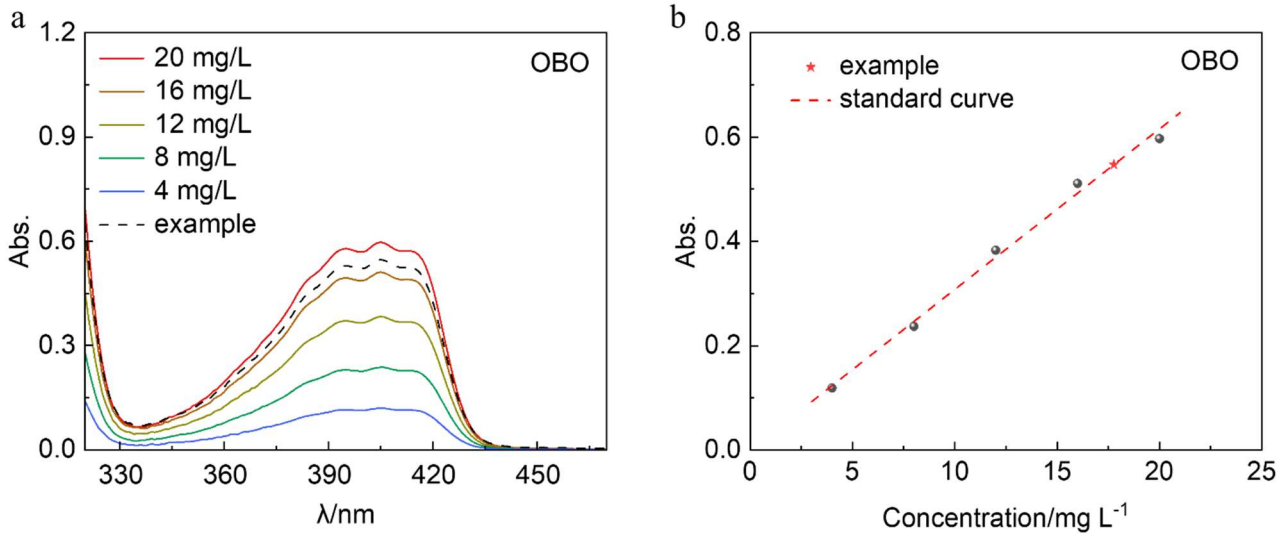

Figure 7. a, b UV-vis spectral characteristic peaks of molecular OBO at various concentrations in acetonitrile, standard curves, and absorbance of diluted samples

The redox properties of OBO was investigated by cyclic voltammetry (CV) using tetrabutylammonium bis-(trifluoromethylsulfonyl)imide (TBA-TFSI) in acetonitrile (ACN) as the electrolyte. As shown in Figure 8, The half-wave potentials at −1.55 and 1.55 V (vs Ag /AgCl) correspond to the reduction and oxidation reactions of OBO, respectively, which is one of the highest voltage for bipolar molecules found so far. Subsequently, we expanded our investigation to assess the redox stability and reversibility of OBO. As shown in Figure 9, within the potential ranges of −1.8 to −1.3 V and +1.15 to +1.65 V (vs Ag/AgCl), OBO exhibited two electrochemically accessible and reversible electron transfer processes with well-defined and symmetrical peaks. The half-wave potentials ($E_{1/2}$) of the two redox processes for OBO were corresponding to the redox events occurring at the B ($E_{1/2}$ ≈ -1.55 V vs Ag/AgCl) and the O ($E_{1/2}$ ≈ 1.55 V vs Ag/AgCl) atoms, respectively. Accordingly, the open-circuit voltage of the symmetric RFBs employing OBO moieties as the active materials is estimated to be 3.1 V. Remarkably, after 100 cycles, the CV curves of OBO molecules nearly overlapped with the initial cycle, demonstrating their high electrochemical stability.

ISSN: 2414-1895 DOI: 10.6919/ICJE.202502_11(2).0019

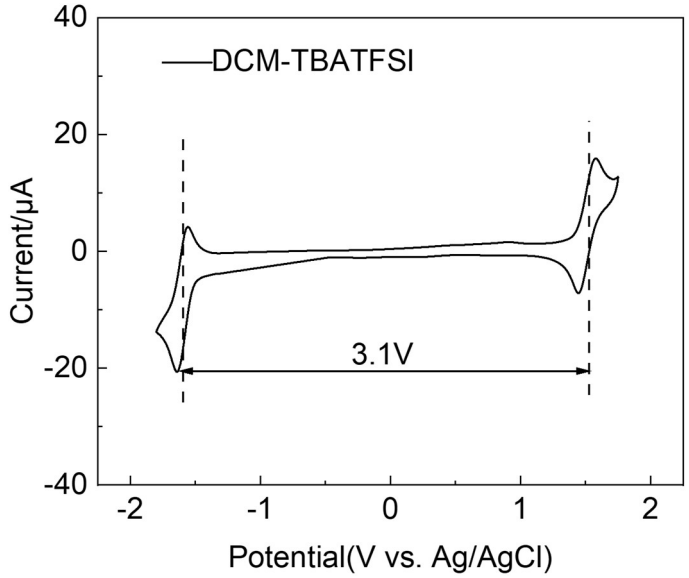

Figure 8. Cyclic voltammetry curves of 1.5 mM OBO in 0.1 M TBATFSI-ACN supporting electrolytes

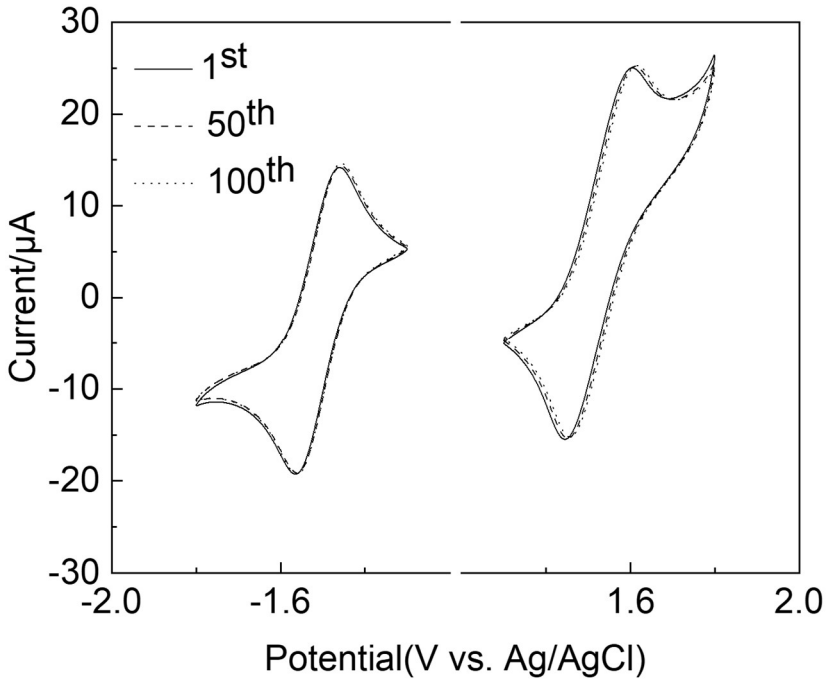

Figure 9. CV profiles of 1.5 mM OBO in 0.1 M TBATFSI-ACN supporting electrolytes, recorded at a sweep rate of 100 mV s^{-1} for the 1st, 50th, and 100th cycles

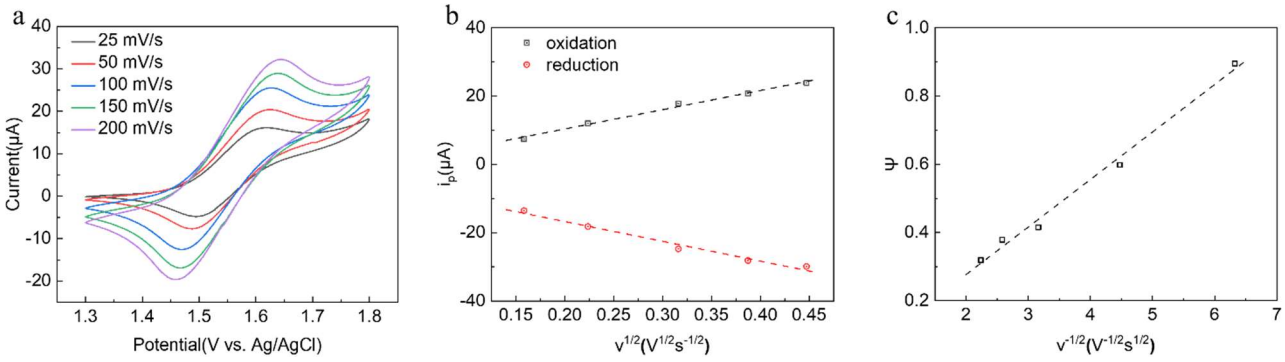

ISSN: 2414-1895 DOI: 10.6919/ICJE.202502_11(2).0019

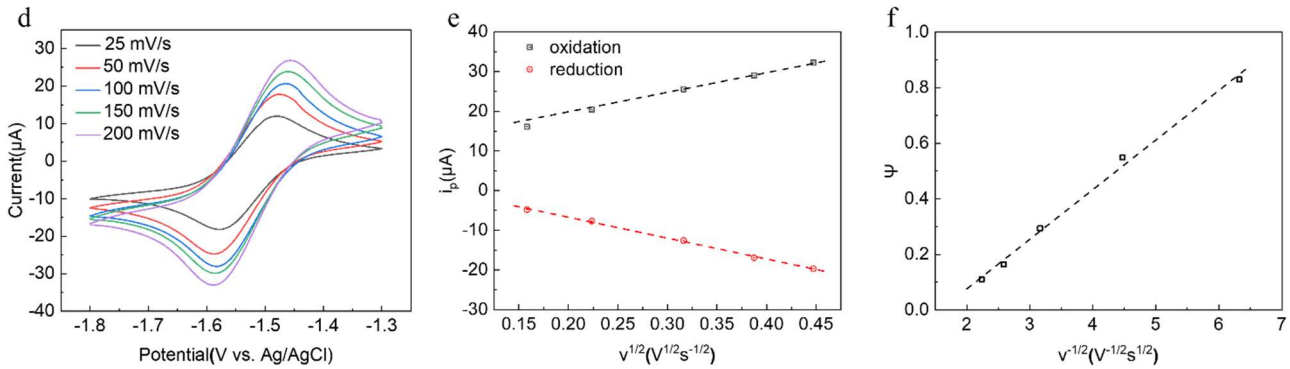

Figure 10. a,d CV curves of cathodic and anodic 1.5 mM OBO in 0.1 M TBATFSI-ACN supporting electrolytes, recorded at scan rates ranging from 25 to 200 mV s^{-1}; b,e Linear fitting plots of the cathodic and anodic peak currents (i_p) for the redox peaks of OBO versus $v^{1/2}$ at various scan rates ranging from 5 to 200 mV s^{-1};) c,f Plots of the cathodic and anodic kinetic parameter Ψ versus the reciprocal of $v^{-1/2}$

We further extended our investigation to elucidate the electrochemical kinetics of the OBO by employing a series of cyclic voltammetry (CV) experiments, with scan rates varying widely from 25 to 200 mV s^{-1}. As shown in Figure 10, both the cathodic and anodic peaks exhibited a high degree of symmetry, and a pronounced linear correlation was discernible between the peak currents and the square root of the scan rate. This suggests that the oxidation and reduction processes are governed by mass-transport-limited redox reactions. The average diffusion coefficient D_0 for the electroactive species OBO was calculated to be 3.52×10^{-6} cm^2s^{-1} employing the Randles-Ševčík equation [6]. Additionally, the heterogeneous electron-transfer rate constants k_0 for the redox couple involving the $[OBO]^+$/OBO and OBO/$[OBO]^-$ species were ascertained using the Nicholson method [7], yielding values of 3.54×10^{-3} cms^{-1} and 3.01×10^{-3} cms^{-1}, respectively. The calculated D_0 and k_0 are similar to the bipolar ROM reported in the literature [8, 9], which indicates the excellent electrochemical kinetic performance of the designed OBO molecule.

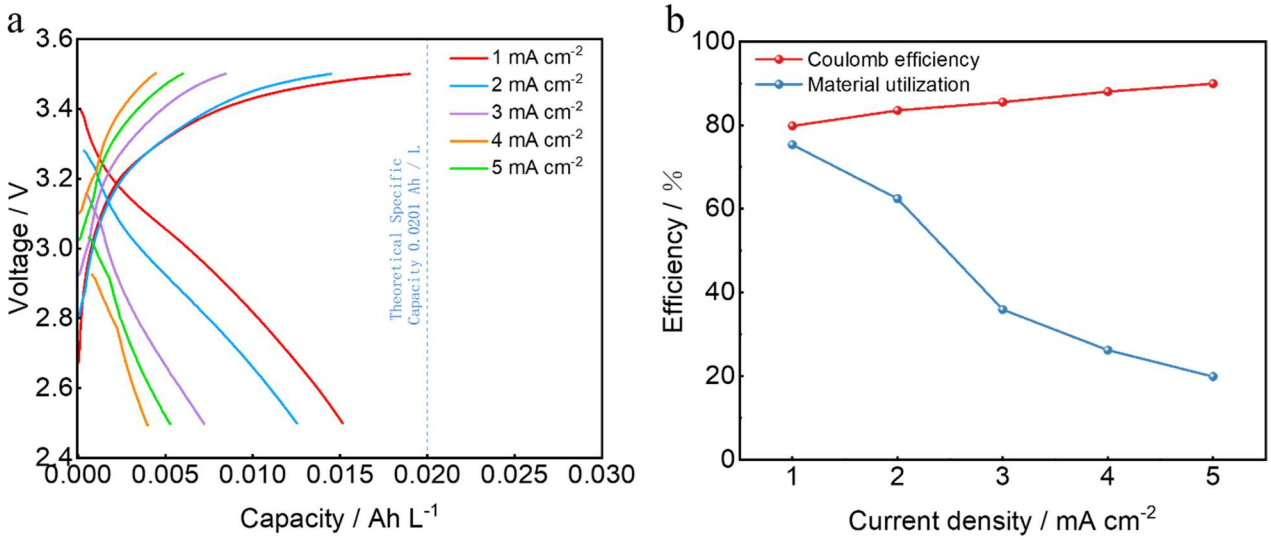

Figure 11. a Typical charge-discharge profiles at varying current densities; b Coulombic efficiency and material utilization of batteries at varying current densities

To assess the practical applicability of OBO molecules, we constructed a flow battery and evaluated its electrochemical performance. Carbon felts were employed as the electrode materials, while a

ISSN: 2414-1895 DOI: 10.6919/ICJE.202502_11(2).0019

Daramic-175 porous membrane functioned as the separator in the flow battery. An acetonitrile (ACN) solution containing OBO and tetrabutylammonium bis(trifluoromethylsulfonyl)imide (TBA-TFSI) was utilized as both the catholyte and anolyte. Equal volumes of 0.1 mL of a 1.5 mM OBO solution in a 0.1 M TBA-TFSI/ACN solvent were introduced into both compartments of the cell, which corresponds to a theoretical capacity of 20.1 mAh L^{-1}. The characteristic charge/discharge profiles, as depicted in Figure 11a, exhibited pronounced plateaus during both charge and discharge processes across all tested current densities. The cell demonstrated its peak active material utilization ratio at approximately 76.2%, with a Coulombic efficiency (CE) of approximately 79.9% and a discharge voltage of approximately 3.05 V at a current density of 1.0 mA cm^{-2}. However, elevating the current density to 3 mA cm^{-2} led to an enhanced Coulombic efficiency (CE) of approximately 82.5% (Figure 11b). This observation is due to the reduced charge-discharge time at elevated currents, which ameliorates the internal shuttle effect through the porous separator. Furthermore, when the current density surpassed 3.0 mA cm^{-2}, a more significant voltage hysteresis effect was observed. This is attributed to concentration polarization, which hampers the mass transport of ions within the electrolyte and through the separator.

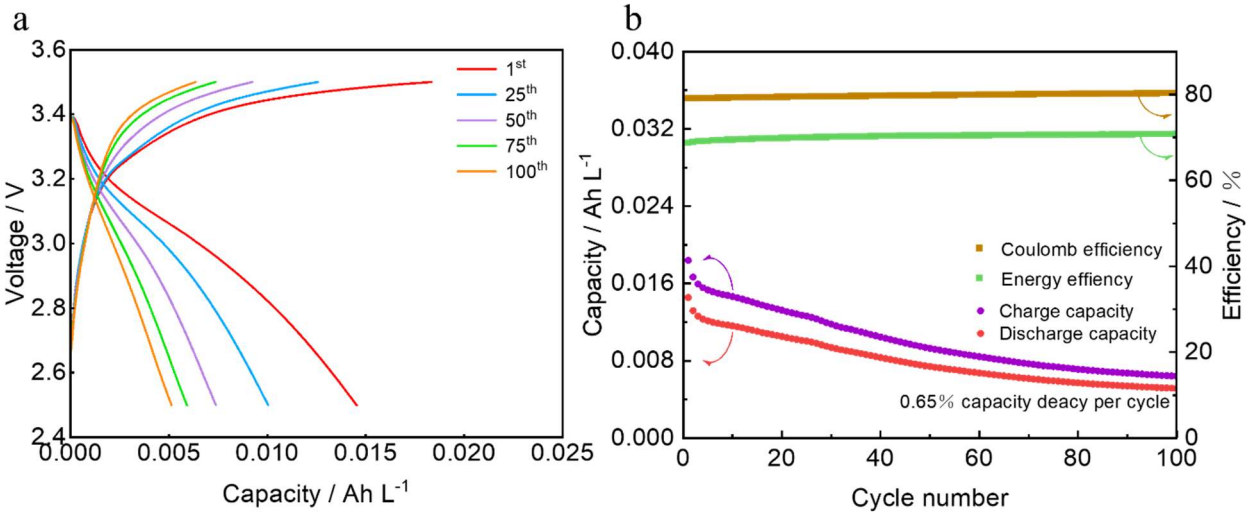

Figure 12. a Selected charge-discharge profiles from long-cycling tests; b along with the corresponding capacity retention, Coulombic efficiency CE and energy efficiency EE at a constant current density of 1.5 mA cm^{-2}

We subsequently evaluated the long-term cycling performance of the OBO-ACN-TBATFSI battery at a current density of 1 mA cm^{-2}. Figure 12a presents the voltage profiles across various charge-discharge cycles, along with the corresponding long-term capacity retention of the static cell. After 100 cycles, the capacity retention of the battery is ca. 35.5%, with the capacity deacy rate of ca. 0.64% per cycle. Moreover, the CE and EE remained above 80% and 70% within 100 cycles (Figure 12b). Nevertheless, due to the low solubility of OBO molecules in acetonitrile, the battery's capacity is relatively low. Future work will focus on further modification and optimization of the OBO molecules to enhance their solubility, thereby increasing the capacity of flow battery.

4. Conclusion

In summary, we have successfully synthesized a novel class of bipolar molecules, OBO, and characterized them using electrochemical cyclic voltammetry (CV) and ultraviolet-visible (UV-vis) absorbance spectroscopy. The assembled flow battery demonstrated high discharge voltage of 3.05 V and excellent CE of 80% and EE of 70% within 100 cycles. Though the capacity of battery being limited by the low molecular solubility, this work presents a novel strategy for constructing bipolar

ISSN: 2414-1895 DOI: 10.6919/ICJE.202502_11(2).0019

redox molecules, offering new insights for the development of next-generation redox flow batteries (RFBs) for energy storage applications.

References

[1] M. Li, J. Case, S.D. Minteer, Bipolar Redox-Active Molecules in Non-Aqueous Organic Redox Flow Batteries: Status and Challenges, ChemElectroChem, vol. 8 (2021), 1215-32.

[2] J. Friedl, M.A. Lebedeva, K. Porfyrakis, et al., All-Fullerene-Based Cells for Nonaqueous Redox Flow Batteries, Journal of the American Chemical Society, vol. 140 (2018), 401-5.

[3] C. Zhang, Y. Qian, Y. Ding, et al. Biredox Eutectic Electrolytes Derived from Organic Redox-Active Molecules: High-Energy Storage Systems, Angew Chem Int Ed Engl, vol. 58 (2019), 7045-50.

[4] K.M. Pelzer, L. Cheng, L.A. Curtiss, Effects of Functional Groups in Redox-Active Organic Molecules: A High-Throughput Screening Approach, The Journal of Physical Chemistry C, vol. 121 (2016), 237-45.

[5] J. Kim, H. Kim, S. Lee, et al. A p–n fusion strategy to design bipolar organic materials for high-energy-density symmetric batteries, Journal of Materials Chemistry A, vol. 9 (2021), 14485-94.

[6] R.S. Nicholson, Theory and application of cyclic voltammetry for measurement of electrode reaction kinetics, Analytical Chemistry, vol. 37 (1965), 1351-5.

[7] R.J. Klingler, Kochi, J. K., Electron-transfer kinetics from cyclic voltammetry. Quantitative description of electrochemical reversibility, The Journal of Physical Chemistry C, vol. 85 (1981), 1731-41.

[8] B. Liu, C.W. Tang, F.K. Sheong, et al. Artificial Bipolar Redox-Active Molecule for Symmetric Nonaqueous Redox Flow Batteries, ACS Sustainable Chemistry & Engineering, vol. 10 (2021), 613-21.

[9] G.S. Nambafu, E.P. Delmo, U. Bin Shahid, et al. Pyromellitic diimide based bipolar molecule for total organic symmetric redox flow battery, Nano Energy, vol. 94 (2022), 106963.